Surgical Oncology 28 (2019) 31–35

Contents lists available at ScienceDirect

Surgical Oncology

journal homepage: www.elsevier.com/locate/suronc

Selection of the respiratory phase in minimally invasive interventions for target registration error minimization

Dominik Spinczyk*, Sylwester Fabian, Krzysztof Król

Silesian University of Technology, Faculty of Biomedical Engineering, 40 Roosevelta, 41-800 Zabrze, Poland

ARTICLE INFO

Keywords:
Reduction of target registration error
Breathing motion
Registration circuits
Elastic body spline
Deformation field

ABSTRACT

Background: In minimally invasive surgery, the main challenge is precisely locating the target during the intervention. For abdominal intervention, one of most important factors causing target motion is breathing. The aim of the study is to efficiently predict target localization during the respiratory in breathing cycle.
Method: Analysis of target registration error (TRE) for the registration circuits method was used to find the breathing phase corresponding to the preoperative Computed Tomography spatial configuration. Then, Elastic Body Spline (EBS) for modeling deformation field and Particle Swarm Optimization method were used to find the desired values of EBS parameters: $\propto$ and stiffness were used.
Results: The proposed methodology was verified during experiments conducted on 21 patients diagnosed with liver tumors. This ability of TRE reduction has been achieved for the respiratory phases founded in registration chain analysis.
Conclusions: The proposed method presents the usability of spatio-temporal analysis of collected real breathing data in order to estimate the position of a target during the respiratory cycle. This method has been developed to perform operations in real-time on a standard workstation.

1. Introduction

In minimally invasive intervention, one of the main challenges is precisely locating the pathological tissue during the intervention. Image-based navigation systems are used to utilize knowledge about the patient's anatomy, acquired on the basis of diagnostic images, during patient therapy. Given the current state-of-the-art, the location of the pathological lesion can be effectively estimated for rigid structures. However, it is a challenge for parenchymal structures [1–4].

The first stage of using the image navigation system is to prepare the patient's anatomical model based on pre-operative images. For this purpose, 3D contrast enhancement Computed Tomography (CT) or Magnetic Resonance Images (MRIs) are usually used. The use of contrast is necessary to effectively differentiate focal lesions. In the case of radio therapeutic protocols, the 4D CT or MRI series are used, which additionally contain information on the mobility of organs and focal lesions during the respiratory cycle. The use of image segmentation algorithms completes this stage, allowing the creation of a personalized anatomy model of the patient containing labels of the segmented anatomical structures and pathological changes relevant to the safety and efficacy of the future surgery. Having a personalized patient anatomy model, the surgeon can plan the potential trajectory of the tool during the procedure - this is the planning stage of the procedure. The most important and at the same time the most difficult stage from the point of view of the effectiveness of the procedure is the stage of supporting the therapy, during which the pre-operative anatomy model of the patient is registered to the patient's position during therapy. Algorithms matching the pre-operative anatomy model of the patient to the position of the patient during the procedure based on the skin markers constitute the main topic of the discussed publication. Quantitative and qualitative evaluation of the fitting process takes place during the procedure. For quantitative evaluation, positioned intraoperative ultrasound images are used where the coverage of the corresponding anatomical structures with pre-operative images is assessed. For quantitative assessment of the registration process, the measure of matching the registered markers in the pre-operative image transferred to the patient's coordinate system - Fiducial Registration Error (FRE) - is used. The Target Registration Error (TRE) measure is used to directly assess the alignment of the focal lesion position during the procedure in relation to the position observed in the pre-operative images. Works based on the so-called the registration circuits presented in the article are based on previous studies that showed an underestimation of the registration error based on a single step. That is why the so-called registration circuits in which the registration process takes place in a few

* Corresponding author.
E-mail address: dspinczyk@polsl.pl (D. Spinczyk).

https://doi.org/10.1016/j.suronc.2018.11.003
Received 5 February 2018; Received in revised form 28 May 2018; Accepted 5 November 2018

List of abbreviation

AQUIRC	Assessing Quality Using Image Registration circuits
CT	Computed Tomography
EBS	Elastic Body Spline
TPS	Thin Plate Spline
FLE	Fiducial Localization Error
FRE	Fiducial Registration Error
H_0	null hypothesis
H_1	alternative hypothesis
MRI	Magnetic Resonance Imaging
PSO	Particle Swarm Optimization
$target_{estim}$	the estimated position of the target point
$target_{real}$	the real position of the target point
TRE	Target Registration Error
ε	dissimilarity measure

steps. The introduction of registration circuits showed that the conducted experiments made it possible to reduce the TRE statistically significantly.

Because the exact location of the tumor during the procedure is not known, this topic is the current area of research. Fitzpatrick proposed a target position estimator [5,6] and found no statistical correlation between FRE and TRE [7]. Datteri in [8] proposed the Assessing Quality Using Image Registration Circuits method (AQUIRC), which measures the quality of registration correlated with the TRE. The algorithm was first presented in [9] and has been used to estimate the quality of the fit for rigid image registration in [10]. The method is based on the idea of registration, which was presented by Woods [11] and Holden [12]. Fitzpatrick [13] proved that using only one chain of registration may lead to underestimation of registration errors. The AQUIRC algorithm uses multiple chains by making modifications to the positions of the markers with estimated Fiducial Localization Error and then making the registration between the modified markers positions. Spinczyk and Fabian [14,15] achieved a significantly smaller value of the median TRE on the basis of deformation using splines and a set of sequential positions of surface markers. They evaluated correlation between FRE and TRE and compared TRE obtained by different registration methods. The best results gave the method, which uses Particle Swarm Optimization in order to calculate the best Elastic Body Splines (EBS) parameters.

The aim of this study is to present the usability of three registration chains used by AQUIRC approach selection of the respiratory phase in minimally invasive interventions. The functionality of TRE reduction has been achieved for the respiratory phases which correspond to optimal phases of 3 registration chains of AQUIRC approach for real data, collected during minimally invasive abdominal surgery interventions.

2. Materials and methods

2.1. The proposed modification of AQUIRC approach

The method presented in this paper, Assessing Quality Using Image Registration Circuits approach, is based on the idea of registration circuits, which was presented by Daterri and Dawant [8]. A registration circuit involves three fiducial configurations A, B, and C and three transformations between them. In their approach, the markers' positions differ between configurations by the assumed localization error. The idea of registration circuits was expanded to multiple circuits (Fig. 1).

In our approach, the configurations' coordinates differ by the markers' positions achieved in the subsequent breathing cycles (Fig. 2).

A graph is constructed for each respiratory phase. Every node represents the set of marker positions achieved in the breathing cycle. N-1 nodes correspond to N-1 observed breathing cycles. The highlighted node represents the set of markers observed in computed tomography performed before the procedure. By arranging marker configurations at the vertices of the graph, we get $\binom{N}{2}$ edges and $\binom{N}{3}$ circuits. In further analysis, those circuits that contain the highlighted node has been considered. A registration circuit whose size is 3 contains three configurations A, B, C and three transformations T_{AB}, T_{BC}, T_{CA}. Points X from configuration A are transformed to X' using those transformations:

$$X' = T_{AB}(T_{BC}(T_{CA}(X)))$$

where:

T_{AB}, T_{BC}, T_{CA} are the transformations between configurations A, B, and C respectively. Transformation between configurations were founded by applying Horn registration on the markers' positions [16].

Each transformation, or edge of the graph, is represented by the dissimilarity measure, ε_A, ε_B, ε_C. The dissimilarity is affected by the registration error of three configurations, i.e., the registration error between A and B, the registration error between B and C, and the registration error between C and A. With only one circuit, the contribution of each component cannot be computed. It can, however, be estimated with more than one circuit. To achieve this, the assumption was made that each registration affects the quality measure multiplicatively:

$$TRE_{circuit\_ABC} = dissimilarity\ (X,\ X') = \varepsilon_A * \varepsilon_B * \varepsilon_c$$

Computing this expression for all possible circuits and rearranging them in matrix form, we obtain:

$$\begin{bmatrix} 1\,1\,1\,0\ldots0 \\ 1\,0\,1\,1\ldots0 \\ 1\,1\,0\,1\ldots0 \\ 0\,1\,1\,1\ldots0 \\ \vdots \end{bmatrix} \begin{bmatrix} \log(\varepsilon_{circuit_1}) \\ \log(\varepsilon_{circuit_2}) \\ \log(\varepsilon_{circuit_3}) \\ \log(\varepsilon_{circuit_4}) \\ \vdots \\ \log\left(\varepsilon_{circuit_{\binom{N}{2}}}\right) \end{bmatrix} = \begin{bmatrix} \log(TRE_{circuit_1}) \\ \log(TRE_{circuit_2}) \\ \log(TRE_{circuit_3}) \\ \log(TRE_{circuit_4}) \\ \vdots \\ \log\left(TRE_{circuit_{\binom{N}{3}}}\right) \end{bmatrix}$$

After solving this system of equations, we obtain error vectors: FRE, TRE, and epsilon, with values in individual vectors corresponding to particular circuits.

2.2. Input data set

In order to analyze the data, the structure of the patient record was designed, which enabled the storage of the required information.

To carry out the registration of marker positions from the position tracking system to Computed Tomography (CT) coordinate system, it is

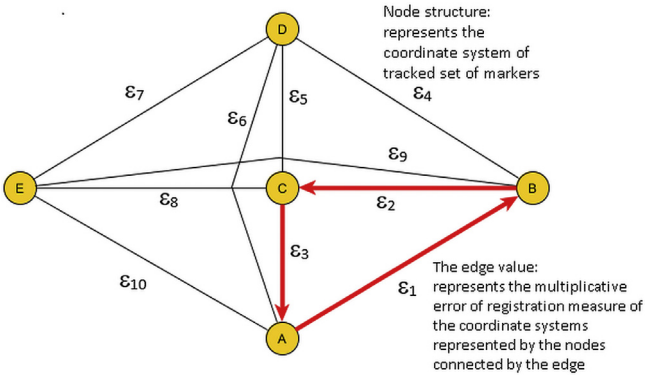

Fig. 1. Example of graph and registration circuit.

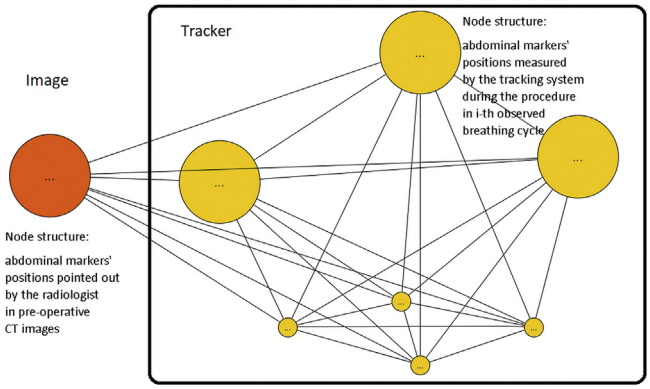

Fig. 2. The presented approach graph.

necessary to determine the position of the corresponding points in both coordinate systems. To specify the position of the markers in the coordinate system associated with the CT images, an application was designed that allows radiologist to review the study, navigate individual cross-sections in any projection, and locate radiological markers and recording their positions in the configuration file.

Depending on the anatomy of the patient (the size of the abdominal area) and previously performed therapy (postoperative scars) on the body, each of the examined patients were had seven to ten sets of correlated radiological markers placed on their abdomen with recognizable markers for the position tracking system (Fig. 3).

After performing a CT scan, a radiologist pointed out position of radiological markers distributed on the body the patient in the computer tomography coordinate system. Because each marker has a three dimensional position, the set of marker positions can be written in a rectangular two-dimensional matrix of $n \times 3$, where n is the number of markers.

After the CT scan, each patient was asked to perform several inhales and exhalations. Accompanying respiratory movement displacement [17] was registered and saved using an application that supports the tracking system. Each position measurement was marked with a time stamp. Based on the analysis of the marker displacements in the Z axis of the tracking system coordinates, the breathing phase $\varnothing_j$ for any time t_j was linearly interpolated [18]:

$$\varnothing_j = \begin{cases} \left(\frac{t_j - t_i^{min}}{t_i^{max} - t_i^{min}}\right)\bar{\varnothing}^{max}\ ;\ dla\ \ t_i^{min} \le t_j < t_i^{max} \\ \bar{\varnothing}^{max} + \left(\frac{t_j - t_i^{max}}{t_{i+1}^{min} - t_i^{max}}\right)(1 - \bar{\varnothing}^{max})\ ;\ dla\ \ t_i^{max} \le t_j < t_{i+1}^{min} \end{cases}$$

$$\bar{\varnothing}^{\max} = \frac{1}{N^{\max}} \sum_{i=1}^{N^{\max}} \frac{t_i^{\max} - t_i^{\min}}{t_{i+1}^{\min} - t_i^{\min}}$$

where:

t_i^{min}, t_i^{max} – time corresponding for i-th minimum and maximum of marker position in Z axis, respectively,
N^{max}– number of acquired breathing cycles.

From the literature [19], it appears that the average cycle length is approximately 4 s. In turn, the maximum sampling frequency of the position tracking system is equal to 25 Hz. Therefore, assuming use modern and efficient hardware architecture, it is possible to collect 100 sets of markers positions in one breathing cycle.

The obtained data set was saved in the patient record in the matrix presented in Fig. 4a. The patient's test record and patient metadata were also recorded in the patient record, which complement the collections of markers positions in time in the tracking system and a collection of markers position in the computed tomography coordinate system. The entire collection of patient records participating in the study has been presented in Fig. 4b.

2.3. Experiment

As it was mentioned earlier, only nodes which include the CT marker positions were included in further analysis. For every marker treated as a target, 50 breathing phases (from 0 to 98% of breathing cycle with step 2%) were selected per every breathing cycle, correspondence graph were built, and the system of equations was solved. Descriptive statistics of TRE, FRE, and epsilon measures have been calculated. The respiratory phase was selected based on the smallest median TRE value. Additionally, the TRE linear correlation coefficient between FRE and epsilon was calculated.

The experimental verification of the proposed methodology was made on the basis of 21 patients diagnosed with liver tumors. At the stage of imaging diagnostics, three-dimensional (3D) computed tomography with contrast was used depending on the adopted acquisition protocol and the potential therapeutic method. In the case of the use of surgical techniques, 3D imaging is most commonly used and the respiratory phase needs to be adjusted. For every patient, each marker was treated as target and the other markers as predictors of target position, which produces 162 configurations and 1095 analyzed breathing cycles.

The results section presents descriptive statistics in the form of TRE box plots calculated as the difference of the actual position of the marker assumed as target, and the position estimated with the Elastic Body Splines deformation field, whose parameters were selected using the Particle Swarm Optimization (PSO) approach. In the *PSO* approach, the dataset consists of available markers positions and configuration recorded for every patient. The dataset has been divided into a training and a test group at a ratio of 50 to 50%. The Training set is used to find the values of ∝ and stiffness parameters (used by the EBS algorithm), in the following way. The values of the parameters in moments of time corresponding to the phase founded in the AQUIRC experiment are averaged for every patient and its markers' configuration independently. Then, those values are used to estimate target position in the test group. A more detailed description of EBS-PSO approach can be found in our previous work [15].

3. Results

After verifying the lack of normal distribution within the analyzed data groups, Wilcoxon's statistical hypothesis test was used in post-hoc analysis to verify differences in distributions within groups connected by the analysis point. The Obtained results in terms of the time criterion (phase in the breathing cycle) were divided into five groups: discrete time moments corresponding to the phase founded in AQUIRC experiment in the breathing cycle, minimum FRE in the breathing cycle, inhale, exhale and full respiratory period.

Fig. 5 shows the distribution of TREs in subgroups determined

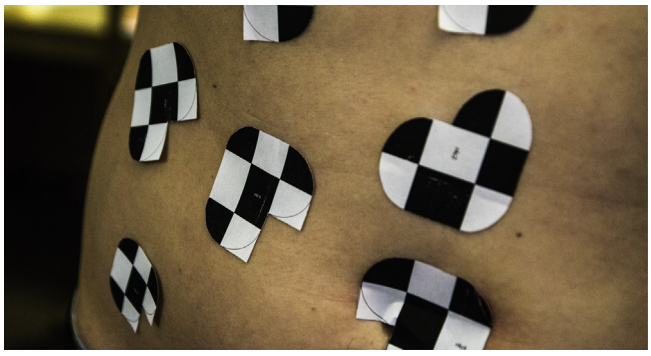

Fig. 3. Placement of markers on the skin.

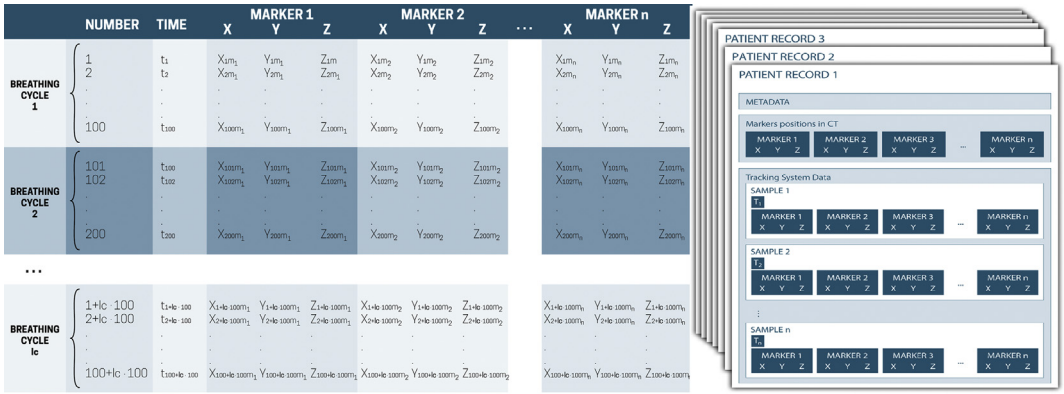

Fig. 4. Matrix of markers with division into cycles (left) and whole data set (right).

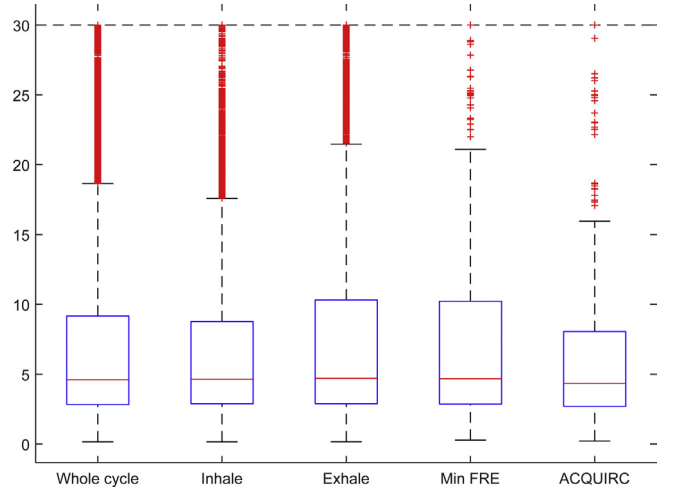

Fig. 5. Distribution of $TRE_{RIGID\text{-}EBS\text{-}PSO}$ estimation with division into groups according to the criterion of the respiratory cycle phase.

according to time criterion.

The lowest median value was obtained for ACQUIRIC group. Therefore, in the further analysis, the median values for the ACQUIREC group were used. Table 1 presents the comparison of median values for ACQUIRIC group for different registration methods evaluated in previous works [14,15].

Table 2 presents comparison of statistical analysis of lower median value of ACQUIRIC group between TRE RIGID-EBS-PSO-ACQUIRIC registration method and other registration method.

4. Discussion

Spatio-temporal analysis of collected real data was performed to estimate the position of target during the respiratory cycle. The Registration circuits method was used to find the breathing phase corresponding to preoperative Computed Tomography spatial configuration. Taking into consideration the time criterion, the data has been divided into 5 groups: discrete time moments corresponding to the phase found in the AQUIRC experiment in the breathing cycles, minimum FRE in the breathing cycle, inhale, exhale and full respiratory period. Minimum FRE group include breathing phase which corresponds to minimum of FRE value for every breathing cycle. This method was described in [15], and until now was the method which produced the best results. This method used Elastic Body Spline for modeling deformation field and Particle Swarm Optimization method to find desired values of EBS parameters: ∝ and stiffness for discrete breathing phase corresponding to minimum FRE in every breathing cycle. In the current approach, in comparison to previous method, we select discrete breathing phases based on TRE analysis of the registration circuits method. It produced statistically better results.

The analysis was performed based on free breathing data collected during the preparation for minimally invasive abdominal surgery. In real clinical scenarios, such interventions are performed in general anesthesia and the breathing process is supervised by a respirator, which causes more regular and repetitive breathing.

There are some limitations to the presented approach. First, to validate the real target position and minimize the invasiveness of the research, fiducial markers were treated as the targets. Therefore, the target was lying on the surface of the abdominal cavity. In the future, a marker placed inside the abdominal cavity will be considered in the proposed approach. Second, experiments on animal tissues during the respiratory cycle showed the effect of the relative position of the markers and the direction of their distribution on the accuracy of TRE estimation [20,21]. Third, another interesting element is the study of the proposed multiplicative error measure of the registration circuit (proposed in [8]) regarding statistical correlation in relation to TRE.

5. Conclusions

In minimally invasive surgery, one of the main challenges is precisely locating the target during the intervention. For abdominal intervention one of most important factor causing target motion is breathing. The aim of the study is to efficiently predict target localization in breathing cycle.

Analysis of TRE for registration circuits was used to find the breathing phase corresponding to preoperative Computed Tomography spatial configuration. Then, Elastic Body Spline for modeling deformation field and Particle Swarm Optimization method were used to find desired values of EBS parameters: ∝ and stiffness. The proposed

Table 1
Median TRE value of ACUIRIC group for different registration methods.

Registration method	Median of TRE [mm]
RIGID	8.31
AFFINE	9.28
AFFINE + THIN PLATE SPLINE	9.28
AFFINE + ELASTIC BODY SPLINE REGISTRATION	8.14
RIGID + THIN PLATE SPLINE	8.31
RIGID + ELASTIC BODY SPLINE	7.60
AFFINE + ELASTIC BODY SPLINE + PARTICAL SWORM OPTIMALIZATION	5.85
RIGID + ELASTIC BODY SPLINE + PARTICAL SWORM OPTIMALIZATION	4.81
RIGID + ELASTIC BODY SPLINE + PARTICAL SWORM OPTIMALIZATION + ACQUIRIC (acronym: ACQUIRIC)	4.34

Table 2
Results of statistical analysis comparing median of TRE for ACQUIRIC group for different registration methods.

Other registration method	Lower median TRE for ACQUIRIC method compared to other registration method
RIGID	YES, p-value = 3,12E-22
AFFINE	YES, p-value = 7,47E-26
AFFINE + THIN PLATE SPLINE	YES, p-value = 7,47E-26
AFFINE + ELASTIC BODY SPLINE REGISTRATION	YES, p-value = 1,88E-25
RIGID + THIN PLATE SPLINE	YES, p-value = 3,12E-22
RIGID + ELASTIC BODY SPLINE	YES, p-value = 2,54E-20
AFFINE + ELASTIC BODY SPLINE + PARTICAL SWORM OPTIMALIZATION	YES, p-value = 7,46E-05
RIGID + ELASTIC BODY SPLINE + PARTICAL SWORM OPTIMALIZATION	YES, p-value = 0,040837

methodology was verified during experiments conducted on 21 patients diagnosed with liver tumors. This functionality of TRE minimization has been achieved for the respiratory phases corresponding to breathing phase found in Image Registration analysis. The proposed method was performed to estimate the position of target during respiratory cycle. This method has been developed to perform operations in real-time on a standard workstation.

Disclosures

Dominik Spinczyk declares no conflict of interest.
Sylwester Fabian declares no conflict of interest.
Krzysztof Król declares no conflict of interest.

Acknowledgments

The method was evaluated based on imaging data of patients from the Second Department of Clinical Radiology and the Department of General, Transplant and Liver Surgery at the Medical University of Warsaw after acceptance by the ethics committee of the Medical University of Warsaw.

We want to thanks Andre Woloshuk for English language corrections.

Appendix A. Supplementary data

Supplementary data to this article can be found online at https://doi.org/10.1016/j.suronc.2018.11.003.

References

[1] S.J. Phee, K. Yang, Interventional navigation systems for treatment of unresectable liver tumor, Med. Biol. Eng. Comput. 48 (2010) 103–111, https://doi.org/10.1007/s11517-009-0568-3 2010.
[2] H. Neshat, D.W. Cool, K. Barker, L. Gardi, N. Kakani, A. Fenster, A 3D ultrasound scanning system for image guided liver interventions, Med. Phys. 40 (2013) 112903, https://doi.org/10.1118/1.4824326 2013.
[3] H.G. Kenngott, M. Wagner, M. Gondan, F. Nickel, M. Nolden, A. Fetzer, et al., Real-time image guidance in laparoscopic liver surgery: first clinical experience with a guidance system based on intraoperative CT imaging, Surg. Endosc. 28 (2014) 933–940, https://doi.org/10.1007/s00464-013-3249-0.
[4] D. Spinczyk, Towards the clinical integration of an image-guided navigation system for percutaneous liver tumor ablation using freehand 2D ultrasound images, Comput. Aided Surg. 20 (2015) 61–72, https://doi.org/10.3109/10929088.2015.1076043 2015.
[5] J.M. Fitzpatrick, J.B. West, C.R. Maurer, Predicting error in rigid-body point-based registration, IEEE Trans. Med. Imag. 17 (1998) 694–702, https://doi.org/10.1109/42.736021 1998.
[6] J.M. Fitzpatrick, J.B. West, The distribution of target registration error in rigid-body point-based registration, IEEE Trans. Med. Imag. 20 (2001) 917–927, https://doi.org/10.1109/42.952729 2001.
[7] J.M. Fitzpatrick, Fiducial registration error and target registration error are uncorrelated, Proc. SPIE 7261, Medical Imaging 2009: Visualization, Image-guided Procedures, and Modeling; 2009, 2009, p. 726102, , https://doi.org/10.1117/12.813601.
[8] R.D. Datteri, B.M. Dawant, Estimation and reduction of target registration error, in: N. Ayache, H. Delingette, P. Golland, K. Mori (Eds.), Medical Image Computing and Computer-assisted Intervention – MICCAI 2012. MICCAI 2012. Lecture Notes in Computer Science, vol. 7512, Springer, Berlin, Heidelberg, 2012, pp. 139–146, , https://doi.org/10.1117/12.911556 2012.
[9] R.D. Datteri, A.J. Asman, B.A. Landman, B.M. Dawant, Estimation of registration quality applied to multi-atlas segmentation, Toronto, Canada, September 2011 (Oral Presentation), 2011 Full Text http://citeseerx.ist.psu.edu/viewdoc/download?doi=10.1.1.728.4212&rep=rep1&type=pdf.
[10] R.D. Datteri, B.M. Dawant, Estimation of rigid-body registration quality using registration networks, Proc. SPIE 8314, Medical Imaging 2012: Image Processing, 2012, p. 831419, , https://doi.org/10.1117/12.911556 , Accessed date: 23 February 2012.
[11] R.P. Woods, S.T. Grafton, C.J. Holmes, S.R. Cherry, J.C. Mazziotta, Automated image registration: I. General methods and intrasubject, intramodality validation, J. Comput. Assist. Tomogr. 22 (1998) 139–152, https://doi.org/10.1097/00004728-199801000-00027 1998.
[12] M. Holden, D.L. Hill, E.R. Denton, J.M. Jarosz, T.C. Cox, T. Rohlfing, J. Goodey, D.J. Hawkes, Voxel similarity measures for 3D serial MR brain image registration, IEEE Trans. Med. Imag. 19 (2000) 94–102, https://doi.org/10.1109/42.836369 2000.
[13] J.M. Fitzpatrick, Detecting failure, assessing success, in: J.V. Hajnal, D.L.G. Hill, D.J. Hawkes (Eds.), Medical Image Registration, CRC Press, Florida, 2001, pp. 117–139 2001.
[14] S. Fabian, D. Spinczyk, Target Registration Error Minimization for Minimally Invasive Interventions Involving Deformable Organs, Comput. Med. Imaging Graph 65 (2018) 4–10 https://doi.org/10.1016/j.compmedimag.2017.01.008.
[15] D. Spinczyk, S. Fabian, Target registration error minimization for minimally invasive interventions involving deformable organs using elastic body splines and Particle Swarm optimization approach, Surgical Oncology, 26 2017, pp. 489–497 2017 https://doi.org/10.1016/j.suronc.2017.09.005.
[16] B.K. Horn, H.M. Hilden, S. Negahdaripour, Closed-form solution of absolute orientation using orthonormal matrices, J. Opt. Soc. Am. A 5 (1988) 1127–1135, https://doi.org/10.1364/JOSAA.5.001127 1988.
[17] Q. Zhang, A. Pevsner, A. Hertanto, Y. Hu, K. Rosenzweig, K. Ling, G. Mageras, A patient-specific respiratory model of anatomical motion for radiation treatment planning, Med. Phys. 34 (2007) 4772–4781 2007.
[18] E. Rijkhorst, D. Heanes, F. Odille, D. Hawkes, D. Barratt, Simulating dynamic ultrasound using MR-derived motion models to assess respiratory synchronization for image-guided liver interventions, Lect. Notes Comput. Sci. 6135 (2010) 113–123 2010.
[19] K. Barrett, S. Boitano, S. Barman, H. Brooks, Ganong's Review of Medical Physiology, Twenty-Third Edition, New York, 2010 2010.
[20] L. Maier-Hein, D. Maleike, J. Neuhaus, A. Franz, I. Wolf, H. Meinzer, Soft tissue navigation using needle-shaped markers: evaluation of navigation aid tracking accuracy and CT registration, SPIE Medical Imaging 2007: Visualization, Image-guided Procedures, and Display, 2007, pp. 6509–650926, , https://doi.org/10.1117/12.707882 2007.
[21] L. Maier-Hein, A. Tekbas, A.M. Franz, R. Tetzlaff, S.A. Müller, F. Pianka, I. Wolf, H.U. Kauczor, B.M. Schmied, H.P. Meinzer, On combining internal and external fiducials for liver motion compensation, Comput. Aided Surg. 13 (2008) 369–376, https://doi.org/10.3109/10929080802610674 2008.